*antibiotics*

MDPI

*Article*

# Can Vitamin B12 Assist the Internalization of Antisense LNA Oligonucleotides into Bacteria?

**Sara Pereira [1], Ruwei Yao [2], Mariana Gomes [1], Per Trolle Jørgensen [2], Jesper Wengel [2], Nuno Filipe Azevedo [1] and Rita Sobral Santos [1,*]**

[1] Laboratory for Process Engineering, Environment, Biotechnology and Energy (LEPABE), Faculty of Engineering, University of Porto, R. Dr. Roberto Frias, 4200-465 Porto, Portugal; up201610825@fe.up.pt (S.P.); mggomes@fe.up.pt (M.G.); nazevedo@fe.up.pt (N.F.A.)

[2] Biomolecular Nanoscale Engineering Center, Department of Physics, Chemistry and Pharmacy, University of Southern Denmark, Campusvej 55, 5230 Odense M, Denmark; ruweiy@kemi.dtu.dk (R.Y.); ptj@sdu.dk (P.T.J.); jwe@sdu.dk (J.W.)

* Correspondence: ritasantos@fe.up.pt

**Abstract:** The emergence of bacterial resistance to traditional small-molecule antibiotics is fueling the search for innovative strategies to treat infections. Inhibiting the expression of essential bacterial genes using antisense oligonucleotides (ASOs), particularly composed of nucleic acid mimics (NAMs), has emerged as a promising strategy. However, their efficiency depends on their association with vectors that can translocate the bacterial envelope. Vitamin $B_{12}$ is among the largest molecules known to be taken up by bacteria and has very recently started to gain interest as a trojan-horse vector. Gapmers and steric blockers were evaluated as ASOs against *Escherichia coli* (*E. coli*). Both ASOs were successfully conjugated to $B_{12}$ by copper-free azide-alkyne click-chemistry. The biological effect of the two conjugates was evaluated together with their intracellular localization in *E. coli*. Although not only $B_{12}$ but also both $B_{12}$-ASO conjugates interacted strongly with *E. coli*, they were mostly colocalized with the outer membrane. Only 6–9% were detected in the cytosol, which showed to be insufficient for bacterial growth inhibition. These results suggest that the internalization of $B_{12}$-ASO conjugates is strongly affected by the low uptake rate of the $B_{12}$ in *E. coli* and that further studies are needed before considering this strategy against biofilms in vivo.

**Keywords:** antibacterial drug; vitamin $B_{12}$; antisense oligonucleotides; nucleic acid mimics; LNA; 2′OMe



**Citation:** Pereira, S.; Yao, R.; Gomes, M.; Jørgensen, P.T.; Wengel, J.; Azevedo, N.F.; Sobral Santos, R. Can Vitamin B12 Assist the Internalization of Antisense LNA Oligonucleotides into Bacteria? *Antibiotics* **2021**, *10*, 379. https://doi.org/10.3390/antibiotics10040379

Academic Editors: Nicholas Dixon and Marc Maresca

Received: 17 February 2021
Accepted: 1 April 2021
Published: 3 April 2021



## 1. Introduction

The emergence of bacterial resistance to traditional antibiotics is considered a major threat in modern medicine [1,2]. Inevitably, innovative research focused on different antibacterial strategies is needed. Antisense oligonucleotides (ASOs) designed to inhibit bacterial gene expression have been gaining increased interest in recent years [3]. ASOs are especially interesting because even if bacteria develop a mutation that renders them resistant (one of the most common forms of resistance), the ASO can be easily redesigned to become an effective antibacterial drug again [4]. ASOs composed of nucleic acid mimics (NAMs), and in particular, locked nucleic acids (LNAs), possess improved target specificity, binding affinity, and resistance to exo- and endonucleases, compared to unmodified RNA or DNA [5,6], and have been successfully tested for clinical applications [7,8]. ASOs can be divided into two major categories, according to their mechanism of action: RNase H competent (or gapmers) and steric blockers (Figure 1). Gapmers are composed of DNA monomers that are typically flanked by LNA or other RNA-mimicking monomers. Upon hybridization of the gapmer to the target mRNA, the RNase H enzyme recognizes the DNA-mRNA heteroduplex and cleaves the target mRNA, leading to its degradation. Alternatively, the hybridization of steric blockers to the target mRNA simply physically

blocks the access of the RNA polymerase to the target mRNA, thus directly inhibiting its translation [9–11]. There is only one study reporting the use of gapmers to target bacteria [11].

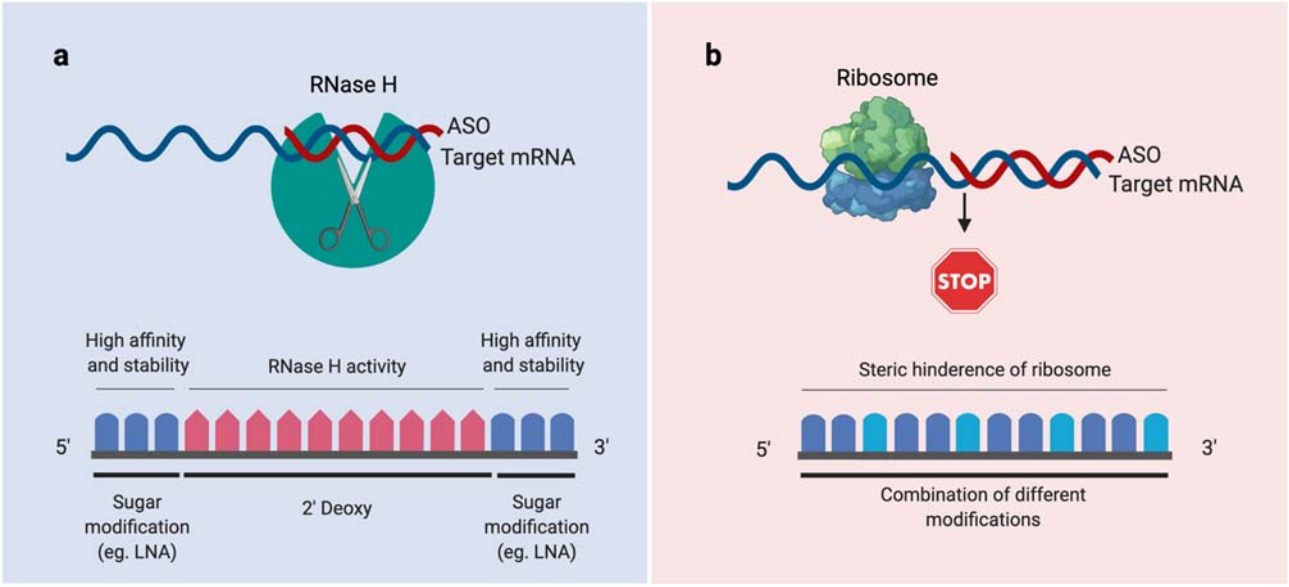


**Figure 1.** Different mechanisms that play a role in the modulation of the RNA function in bacteria. (**a**) Upon hybridization of a gapmer (red), the RNase H is recruited, and the target is degraded. (**b**) Steric hindrance of the ribosome caused by the hybridization between a steric blocker (red) and the complementary mRNA sequence. Figure created using BioRender.

Nonetheless, the use of ASOs is limited by their inability to efficiently penetrate the complex envelope of bacteria. To overcome this burden, delivery vectors mostly focused on cell-penetrating peptides (CPPs) have been investigated. However, CPPs have been almost exclusively conjugated to neutral NAMs, such as peptide nucleic acids (PNAs) or phosphorodiamidate morpholino oligos (PMOs), which might present cytotoxicity and solubility issues [12–14]. Due to chemical conjugation difficulties, the vectorization of anionic ASOs with CPPs has been hampered. In a different approach, vitamin $B_{12}$ ($B_{12}$ or cobalamin), one of the largest molecules known to be taken up by bacteria, can be considered as a trojan-horse vector for neutral as well as anionic ASOs. The uptake system of $B_{12}$ has been mostly studied in *E. coli*. [15]. *E. coli* uptakes $B_{12}$ through the outer-membrane β-barrel protein BtuB in a TonB-dependent manner [16]. In the periplasm, BtuF binds to and delivers $B_{12}$ to the ABC-type transporter BtuCD in the inner membrane, which, in turn, transports $B_{12}$ into the cytoplasm [17,18].

Several functional groups are available for the modification of $B_{12}$ to allow conjugation with ASOs, but not all modification sites are suitable to sustain their recognition and uptake [19]. Chromiński et al. described for the first time the synthesis of a clickable $B_{12}$ derivate, possessing an azide functionality at the 5′ end [20]. This modification has already been tested for the copper-dependent conjugation of $B_{12}$ with oligonucleotides, either composed of PNA or 2′OMe, mainly to inhibit genes that code for reporter proteins such as the red fluorescent protein (RFP) [6,20,21]. To our knowledge, there is only one study where a $B_{12}$ conjugate was studied to decrease bacterial growth by inhibition of the essential gene *acpP* in *E. coli* using a PNA ASO [22]. This $B_{12}$-PNA conjugate was only proved to inhibit *E. coli* growth in a very specific medium named Scarlett and Turner [22]. Under these conditions, even in the absence of $B_{12}$ conjugates, bacteria only started growing after 48 h, while in other common minimal media, the exponential growth starts already after 5 h [23].

Occasionally, infections are associated with the formation of biofilms, adding an extra barrier for the use of antibacterial compounds [24]. ASOs were already shown to prevent biofilm formation and reduce mature biofilms, using either peptide nucleic acids (PNAs) or

phosphorodiamidate morpholino oligomers (PMOs) as NAMs, conjugated to CPPs [25,26] but, to the best of our knowledge, never conjugated to $B_{12}$. However, and because the cytosol is the ultimate target for these conjugates, it is important to first investigate their single-cell internalization.

In this study, we have investigated, for the first time, the internalization and inhibition efficiency of two different copper-free clicked conjugates, composed of vitamin $B_{12}$ linked to LNA-based ASOs: a gapmer and a steric blocker. Both ASOs were designed to target the *acpP* gene in *E. coli*, which codes for an essential protein involved in fatty acid biosynthesis [27].

## 2. Results and Discussion

### *2.1. Conjugation of ASOs with Vitamin $B_{12}$*

In this study, two different kinds of LNA antisense oligonucleotides were designed and synthesized to target the *acpP* gene in *E. coli* (Figure 2a): an LNA/DNA gapmer ($ASO_{gapmer}$) and an LNA/2′OMe steric blocker ($ASO_{steric}$) [28,29]. While steric blockers have been widely tested in bacteria [4,27,30–32], gapmers have been mostly studied in mammalian cells [11]. As such, we intended to compare the potency of the different antisense mechanisms in *E. coli.* As the bacterial envelope poses a stringent barrier to the internalization of oligonucleotides, appropriate vectors must be applied for their transport into the bacterial cytosol. This is the first study documenting the use of $B_{12}$ as a vector for LNA oligonucleotides. For the association of $B_{12}$ to $ASO_{steric}$ and $ASO_{gamper}$, a copper-free ring-strain-promoted azide-alkyne coupling reaction was used (Figure 2b) [33]. This method proved to be efficient and resulted in satisfactory yields (Table S1). The increase in HPLC retention time for the $B_{12}$-$ASO_{gamper}$ and $B_{12}$-$ASO_{steric}$ compared with the $ASO_{gapmer}$ and $ASO_{steric}$ points toward efficient conjugation, confirmed by the obtained molecular masses, which are similar to the calculated theoretical values (Figure S1). The conjugation yields were determined as 70% and 97%, respectively, for $B_{12}$-$ASO_{gamper}$ and $B_{12}$-$ASO_{steric}$.

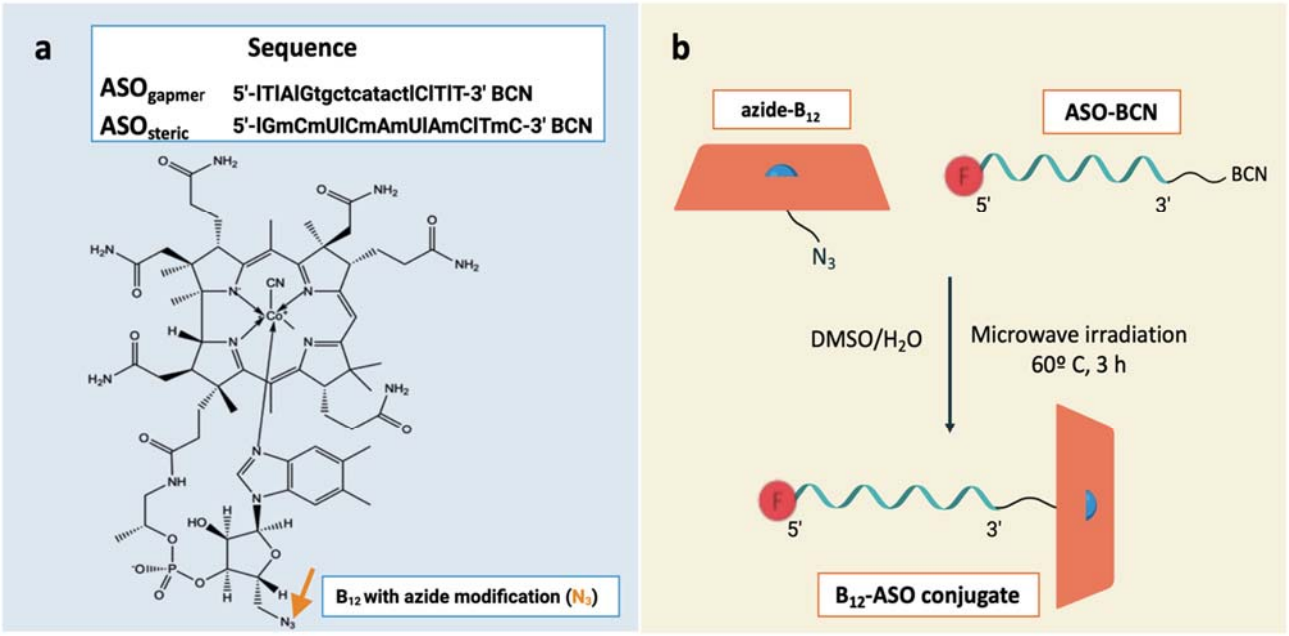


**Figure 2.** $B_{12}$ and antisense oligonucleotides (ASOs) conjugation: sequences and structures. (**a**) Sequence of the $ASO_{gapmer}$ and the $ASO_{steric}$ (LNA nucleotide monomers are represented with upper case letters preceded by l, 2′OMe monomers are represented with upper case letters preceded by m, and DNA monomers are represented by lower case letters) and structure of 5′-end azide-modified $B_{12}$ used in this study. The arrow points to the region of conjugation. (**b**) Schematic illustration of the synthesis of the $B_{12}$-ASO conjugates through copper-free azide-alkyne chemistry.

### 2.2. Bacterial Susceptibility Tests

Both ASOs were designed to recognize the *acpP* essential gene in *E. coli* and thus inhibit its expression. This should result in decreased *E. coli* viability, as long as the ASOs conjugated to $B_{12}$ can efficiently penetrate the bacterial envelope. We investigated the ability of both conjugates ($B_{12}$-$ASO_{gapmer}$ and $B_{12}$-$ASO_{steric}$) to inhibit the growth of *E. coli* in Davis minimal medium at a concentration of 30 μM. This concentration was selected based on the good inhibition efficiency of a cell-penetrating peptide (CPP) conjugated with PNA, targeting the same gene (Figure 3, orange line). Our results show no inhibition using either conjugate composed of $B_{12}$ at the same concentration (Figure 3).

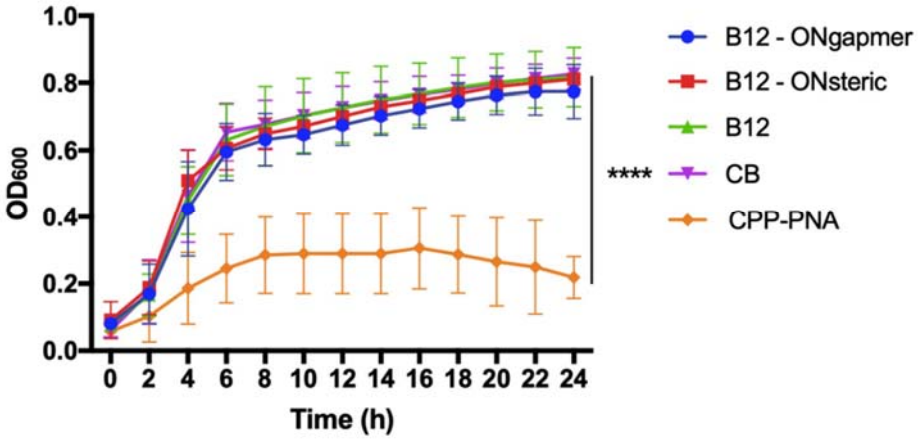


**Figure 3.** Growth of *E. coli* K12 in Davis minimal medium supplemented with $B_{12}$-$ASO_{gapmer}$, $B_{12}$-$ASO_{steric,}$ and $B_{12}$ (at a concentration of 30 μM). CB represents the bacterial growth control in medium without any supplementation. Growth inhibition of *E. coli* K12 using a cell-penetrating peptide conjugated with an ASO composed of peptide nucleic acids (PNAs) (cell-penetrating peptides (CPP)-PNA) at a concentration of 30 μM is also shown. Results from three independent experiments (using duplicates in each) are presented as mean values and respective standard deviations. Statistical differences are indicated when appropriate in * ($p \leq 0.0001$, ****).

In previous studies, PNA and 2′OMe steric blockers conjugated to $B_{12}$ were able to decrease by 1-fold the expression of red fluorescence protein (RFP) in *E. coli* in Davis minimal medium [6,21]. However, to our knowledge, there is no other study including a regular growth control where $B_{12}$-ASOs were investigated to kill bacteria, targeting an essential gene rather than a report protein. The only existing study uses a $B_{12}$-PNA ($ASO_{steric}$ targeting *acpP*) against *E. coli* in a particular medium where the control bacteria only starts growing after 48 h [22]. Nonetheless, the activity of this ASO sequence is already well established, as growth inhibition of *E. coli* K12 has been repeatedly reported using CPP-PNA [27,34,35], which was also confirmed herein. It is clear from the growth curves that the internalization occurs using the CPP as a vector for ASOs, as opposed to the $B_{12}$ vector.

The lack of inhibitory effect of the *E. coli* K12 growth, observed with the conjugates synthesized in the present work, raises the question if the conjugates were efficiently internalized in the bacterial cells. In order to answer this question, location studies were performed next.

### 2.3. Evaluation of the Internalization of $B_{12}$-ASOs

To examine the internalization of both conjugates in *E. coli* K12 and assess if association of the ASOs to the $B_{12}$ could have hampered $B_{12}$-promoted uptake, bacteria were observed under an epifluorescence microscope, after incubation with each of the Cy3-labeled conjugates or controls ($B_{12}$, $ASO_{gapmer,}$ and $ASO_{steric}$).

As expected, almost no fluorescent bacteria were detected when $ASO_{gapmer}$ and $ASO_{steric}$ were used alone (Figure 4–$ASO_{gapmer}$ and $ASO_{steric}$, Cy3 line). In contrast, it is

clear that the conjugation of $B_{12}$ to either ASO significantly increased the amount of fluorescently labeled *E. coli* K12, with all cells becoming fluorescent (Figure 4, $B_{12}$-$ASO_{gapmer}$ and $B_{12}$-$ASO_{steric}$). The same was observed for the $B_{12}$ control (Figure 4, $B_{12}$). Figure 4 shows images obtained at 30 μM, but a similar pattern was obtained for the lower concentration tested (15 μM, Figure S2).

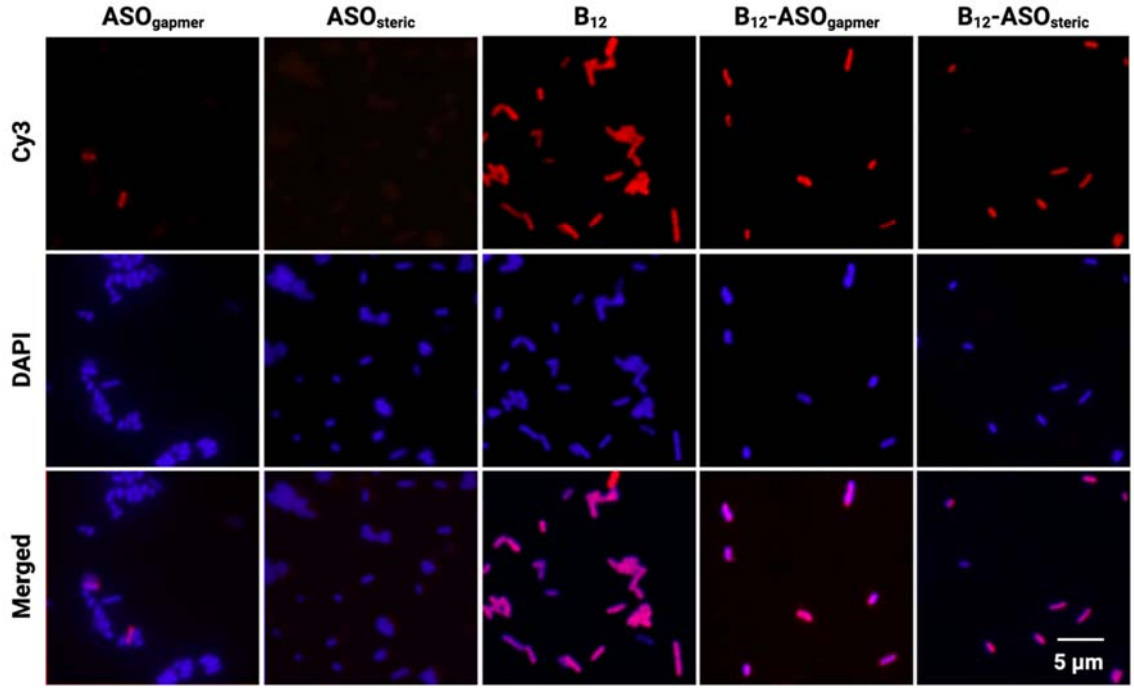


**Figure 4.** Interaction of Cy3-labeled ASOs, $B_{12}$, and $B_{12}$ conjugates (concentration of 30 μM) with *E. coli* K12 after 4 h. Bacteria are counterstained with 4′,6′-diamidino-2-phenylindole (DAPI). Images are representative of three independent experiments (using duplicates in each). Scale bar represents 5 μm.

These results point toward the $B_{12}$-promoted association of the conjugates with the bacterial cells. However, the experimental distinction between membrane-associated and internalized molecules in bacteria remains a difficult task, given the small size of bacteria, which challenges the resolution limit of most standard equipment, including fluorescence microscopes [36].

Therefore, in an attempt to understand if the conjugates were internalized or membrane adhered, as well as to quantify their relative distribution, the bacterial cells were fractionated. A series of washing steps with a gradient of Triton X-100 concentrations was used to differentiate the membrane fraction from the cytosol [37]. These fractions were quantified using a fluorometer. Figure 5 clearly shows that only a small fraction of $B_{12}$ and $B_{12}$ conjugates completely penetrate the bacterial envelope into the cytosol (only 12%, 9%, and 6%, respectively, for the unconjugated $B_{12}$, $B_{12}$-$ASO_{gapmer}$, and $B_{12}$-$ASO_{steric}$), while more than 80% remain adhered to the membrane in all cases. The presence on the periplasm is not relevant (only ~3% of the conjugates were retained in this matrix, which was not statistically different from the cytosol. $p > 0.05$, Figure S3 [38]), which indicates that the BtuB at the outer membrane (OM) is likely the limiting factor for conjugate internalization into the cytosol. On the contrary, 4′,6′-diamidino-2-phenylindole (DAPI), a small and cell-permeant DNA intercalating dye, was majorly localized at the cytosol (Figure 5), as expected. Nonetheless, a small fraction was also present in the membrane (Figure 5), which can occur especially in non-fixed cells [39].

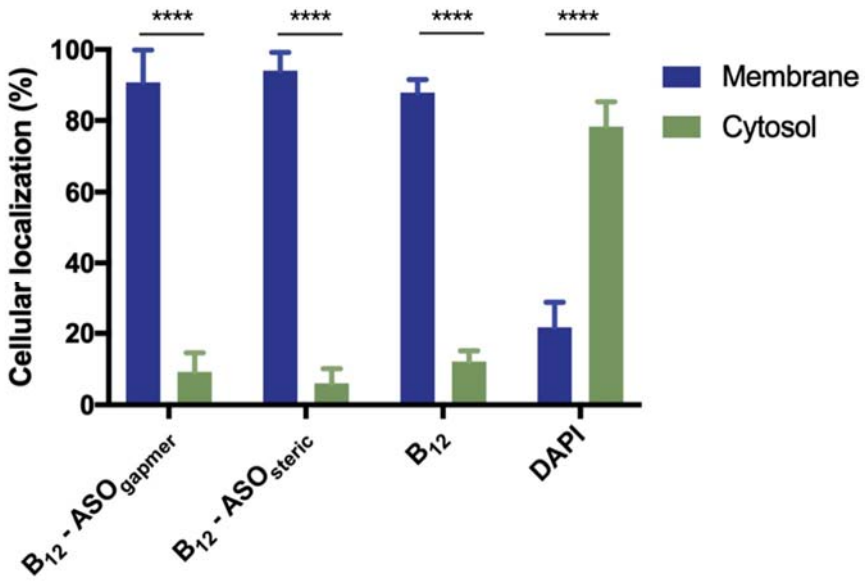


**Figure 5.** Cellular localization of $B_{12}$ conjugates, $B_{12}$, and DAPI control in *E. coli* K12. $B_{12}$ conjugates and $B_{12}$ are mainly found on the OM, while the DAPI control is mostly associated with the cytosol. No significant differences were observed between the different internalized conjugates and between the conjugates and the $B_{12}$ control ($p > 0.05$). Significant differences were observed between the membrane and cytosol-associated compounds ($p \leq 0.0001$, ****). The fluorescence of each fraction present in the DAPI control is significantly different from the tested counterparts ($p \leq 0.0001$). Results are presented as mean values and respective standard deviation from three independent assays (using duplicates in each).

From the obtained fractionation results, it can be concluded that the microscopy fluorescence observed in Figure 4 is predominantly derived from conjugates associated with the OM of *E. coli* K12, rather than conjugates internalized in the cytosol, where the ASO would hybridize the *acpP* mRNA target. The inability of $B_{12}$ to serve, in this study, as an efficient trojan-horse for the internalization of ASOs explains the lack of antimicrobial activity of the conjugates observed in Figure 3. It is possible that the uptake of $B_{12}$ is strongly limited by the activity of BtuB, which is present in the OM.

The uptake of $B_{12}$ is regulated by the expression/repression of the BtuB, the locus encoding for the $B_{12}$ receptor [40]. $B_{12}$ acts as a cofactor for methionine synthesis, necessary for growth [41]. In *E. coli*, it has been estimated that the methionine synthesis requires very low levels of $B_{12}$ (20 molecules per cell) [42], while there are hundreds of thousands of mRNA copies of the *acpP* gene [43]. In our work, we have used a much higher concentration of $B_{12}$ than the amount that *E. coli* needs for methionine synthesis. Hence, the difference between the amount of internalized $B_{12}$ conjugates and the high amount of copies of the essential gene we aimed to inhibit may explain the lack of effectiveness of the conjugates.

In addition, it is also important to reflect on the future of this strategy, considering that in vivo, the number of internalized conjugates will probably be even lower since the host cells, as well as other bacteria from the microbiome, will compete for $B_{12}$. Moreover, most in vivo infections are associated not with single-cell but with clustered cells organized in biofilms [44,45]. Therefore, the bioavailability of $B_{12}$ conjugates may also be limited by interactions with the extracellular matrix. Nonetheless, genes encoding for virulent characteristics, such as the biofilm formation, are usually present in lower amounts of copies. Thus, it would be relevant to study the effect of $B_{12}$-ASO conjugates targeting these genes in the future. In addition, the in vivo competition for $B_{12}$ will favor bacteria with an improved affinity toward $B_{12}$, as it has been found for some bacteria in the gut possessing an additional lipoprotein (BtuG) [46]. The use of $B_{12}$ conjugates to target infections caused by such bacteria possessing BtuG could be considered in future biofilm studies.

## 3. Materials and Methods

### *3.1. Materials*

All basic reagents used were purchased from commercial sources (Sigma-Aldrich, Søhus, Denmark) and used as received. Specific reagents and chemicals included LNA phosphoramidite monomers (Innovassynth Technologies, Maharashtra, India), DNA phosphoramidite monomers (Sigma-Aldrich, St Louis, MO, USA), 2′OMe phosphoramidite monomers, 3′-PT-amino-modifier C6, BCN *N*-hydroxysuccinimide ester (Glen Research, Sterling, VA, USA), DBCO-sulfo-Cy3 (Jena Bioscience, Jena, Germany) and Vitamin $B_{12}$ (Carbosynth, Compton, U.K).

### *3.2. Synthesis and Design of the ASOs*

ASOs were designed to target the gene *acpP*, an essential gene coding for a protein involved in fatty acid biosynthesis. The particular *acpP* target region for the ASOs was selected based on previous studies [22,27,47]. Two different ASOs were synthesized: (i) an LNA/2′OMe chimera, designed for steric blocking ($ASO_{steric}$), and (ii) an LNA/DNA chimera ($ASO_{gapmer}$), designed to recruit RNase (sequences are represented in Figure 1a). Since LNA and 2′OMe substitutions increase the duplex stability, the $ASO_{steric}$ was designed to be shorter than the $ASO_{gapmer}$. ASOs were synthesized under anhydrous conditions using a PerSpective Biosystems Expedite 8909 nucleic acid synthesizer, as described elsewhere [48]. The synthesis was performed on a 1 µmol scale, using a 3′-PT-amino-modifier C6 support, with the following conditions: trichloroacetic acid in $CH_2Cl_2$ (3:97) as detritylation reagent, 0.25 M 4,5-dicyanoimidazole (DCI) in $CH_3CN$ as an activator, acetic anhydride in THF (9:91, *v*/*v*) as cap A solution, *N*-methylimidazole in THF (1:9, *v*/*v*) as cap B solution, and a thiolation solution containing 0.0225 M xanthan hydrate in pyridine/$CH_3CN$ (20:90, *v*/*v*). The coupling time was 4.6 min for both monomers. To obtain labeled ASOs, Cy3 phosphoramidite was added to the 5′ end in anhydrous $CH_3CN$ (0.1 M) and activated by tetrazole with a 15 min coupling time. The stepwise coupling yields were determined by the UV absorbance (at 500 nm) of dimethoxytrityl cations ($DMT^+$) that were released after each coupling. The resulting ASOs were purified by reverse-phase HPLC (RP-HPLC), using a Waters System 600 HPLC equipment, equipped with a Waters XBridge BEH C18-column (5 µm, 100 nm × 19 mm). Their composition and purity (>85%) were confirmed by MALDI-TOF MS and ion-exchange HPLC analysis, respectively. Finally, the purified ASOs were labeled by reaction with BCN *N*-hydroxysuccinimide ester I in carbonate buffer (ASO:BCN = 1:2.5 equivalent) for 2 h. BCN labeled ASOs were desalted using NAP-10 Sephadex columns and purified by RP-HPLC. Their composition and purity (>95%) were confirmed by MALDI-TOF MS and analytical reverse-RP-HPLC, respectively. Concentrations of purified oligonucleotides were determined by UV absorption measurements at 600 nm.

### *3.3. Conjugation of ASOs with Vitamin $B_{12}$*

The 5′-azide-$B_{12}$ was synthesized from commercially available vitamin $B_{12}$ as described by Chromiński et al. [20]. Briefly, the 5′-hydroxy group of the $B_{12}$ was transformed into a good leaving group (a mesyl group), and subsequently, azidation reaction provided the desired 5′-azide-$B_{12}$. The 5′ position was chosen to avoid obstruction of both components of the conjugate [6]. The azide-$B_{12}$ was isolated through precipitation. MS and NMR data were in accordance with the reported data [20].

Each Cy3-labeled ASO-BCN, dissolved in Milli-Q water, was added to a solution of azido-$B_{12}$, dissolved in DMSO (ASO: azido-$B_{12}$ = 1:2 equivalent). The resulting solution was transferred to a Biotage microwave reaction vial (0.5 mL) and sealed under a nitrogen atmosphere. The reaction was carried out on a Biotage Initiator microwave synthesizer at 60 °C for 3 h, whereupon all solvents were removed in vacuo, and the residue was re-dissolved in Milli-Q water (Figure 1b). Analytical RP-HPLC and MALDI-TOF MS were performed. The resulting solutions were de-salted by precipitation of the products by first adding an aqueous solution of sodium acetate (3 M, 15 µL) followed by the addition of

cold ethanol (1 mL, 99% *w*/*w*; −20 °C). The resulting suspensions were stored at −20 °C for 1 h, and after centrifugation (16,000× *g*, 5 min, 4 °C), the supernatants were removed, and the pellet further washed with cold ethanol (2 × 1 mL; −20 °C), dried for 2 h and then dissolved in Milli-Q water (1 mL). Mass spectra of $B_{12}$-ASO conjugates were recorded using MALDI-TOF MS, and the purity was confirmed by analytical RP-HPLC. Concentrations of purified conjugates were determined by ultraviolet absorbance at 260 nm.

The same procedure was conducted to obtain fluorescently labeled $B_{12}$ (without ASO) where DBCO-sulfo-Cy3, instead of the Cy3-labeled ASOs, was conjugated to $B_{12}$ through click-chemistry.

### *3.4. Bacterial Strain and Growth Conditions*

*E. coli* K12 MG1655 was used in this study. To prepare the inoculum, the strain was grown overnight in tryptic soy broth (TSB) at 37 °C with shaking (180 rpm). To monitor both the inhibition of the *acpP* gene expression and the location of the conjugates, *E. coli* K12 was grown in Davis minimal medium at 37 °C with shaking (180 rpm) [49]. This medium lacks $B_{12}$ in its composition, which was crucial to ensure that the internalized $B_{12}$ comes from the control/conjugates incubated with bacteria [6,21].

### *3.5. Bacterial Susceptibility Tests*

The inhibition of the expression of the essential *acpP* gene by the conjugates $B_{12}$-$ASO_{gapmer}$ and $B_{12}$-$ASO_{steric}$ was evaluated by monitoring the growth of *E. coli* K12, using a standard microdilution method. An overnight culture of *E. coli* K12 was diluted to an $OD_{600}$ of 0.1 in fresh Davis minimum medium. These cell suspensions were added to wells of sterile 96-well plates and incubated with different concentrations of the tested compounds at 37 °C. The final concentration of the $B_{12}$-ASOs and respective controls ($B_{12}$, $ASO_{gapmer,}$ and $ASO_{steric}$) was 30 µM. As a control for the ASOs activity, the most well-studied vector-ASO conjugate was tested. In brief, a conjugate composed of the cell-penetrating peptide $(KFF)_3K$ and peptide nucleic acid (PNA) (Eurogentec, Seraing, Belgium), designed to hybridize with the same *acpP* sequence was tested in the same conditions as the $B_{12}$ conjugates. The absorbance at 600 nm was determined on a BMGLabtech SPECTROstar Nano microplate reader for 24 h. *E. coli* in medium without any added compound was used as control (CB). Experiments were performed in three independent biological replicates.

### *3.6. Evaluation of the Internalization of $B_{12}$-ASOs by Epifluorescence Microscopy*

To evaluate the extent of internalized $B_{12}$-ASO conjugates, compared with the ASOs alone, we used epifluorescence microscopy. An overnight culture of *E. coli* K12 was diluted to an $OD_{600}$ of 0.1 in fresh Davis minimum medium. The $B_{12}$-$ASO_{gapmer}$, $B_{12}$-$ASO_{steric}$, $B_{12}$, $ASO_{gapmer,}$ and $ASO_{steric}$ (all Cy3-labeled) were diluted in sterile distilled $H_2O$ and added to the bacterial suspension to a final concentration of 15 and 30 µM per test tube. After 4 h incubation, tubes were centrifuged (3000× *g*, 10 min), and the pellets were resuspended in sterile distilled $H_2O$. To label the bacterial cytosol, 4′,6′-diamidino-2-phenylindole (DAPI) staining was used. Staining was performed by placing a drop of DAPI (0.5 µg/mL) on top of the dried sample for 5 min. The samples were visualized on a Nikon Eclipse T*i* SR epifluorescence microscope using a Nikon Plan-Apo 100X objective. Ten pictures of each sample were taken randomly, covering all the areas of the sample, using a QImaging Retiga R1 monochromatic camera, and processed with the NIS-Elements Advanced Research. The exposure time and the excitation intensity were maintained throughout the experiments. A G-2A longpass filter (excitation: 535 nm; emission: 580 nm) and a DAPI bandpass filter (excitation: 375 nm; emission: 460 nm) were used. The images obtained using both filters were merged using the Fiji software. Three repeated samples were analyzed for each condition, and three independent experiments were performed.

### *3.7. Evaluation of the Internalization of $B_{12}$-ASOs by Bacterial Fractionation*

To determine the location of the conjugates in the *E. coli* K12 cells visualized in the previous section and investigate if the observed fluorescence could derive from association to the bacterial envelope, as opposed to intracellular hybridization, the cells were fractionated, and the fluorescence of the outer-membrane fraction and periplasm vs. the fluorescence of the cytosol fraction was measured.

An overnight inoculum of *E. coli* K12 was diluted to an $OD_{600}$ of 0.1 and grown in Davis minimal medium in the presence of 30 μM of $B_{12}$-$ASO_{gapmer}$, $B_{12}$-$ASO_{steric,}$ and $B_{12}$, (all Cy3-labeled) for 4 h. Thereafter, a fractionation protocol (Figure 6) adapted from Banbula et al. [50] was followed. In brief, bacteria were centrifuged (3000× *g*, 20 min), resuspended in 10 mM Tris-150 mM NaCl (pH 7.4), and washed with 50 mM Tris (pH 7.6). To obtain the fraction associated with the outer-membrane (membrane fraction), bacteria were centrifuged (3000× *g*, 20 min) and resuspended in 50 mM Tris buffer solution containing 0.05% Triton X-100 (pH 7.6), for 1 h at room temperature (RT). After new centrifugation (same conditions), the Cy3 fluorescence intensity of the supernatant (membrane fraction) was measured with a fluorometer (BMGLabtech Fluorostar Omega), using 550 nm excitation and 570 nm emission filters. To obtain the fraction associated with the cytosol, the pellet was resuspended in a more astringent buffer containing 50 mM Tris 1% Triton X-100 (pH 7.6), for 1 h at RT. The supernatant resultant from the last centrifugation was removed, and the Cy3 fluorescence of the cytosol (cytosol fraction) was measured. As a control, the same fractionation protocol was applied to bacteria stained only with DAPI, and the fluorescence of the membrane and cytosol fractions was measured using 375 nm excitation and 460 nm emission filters.

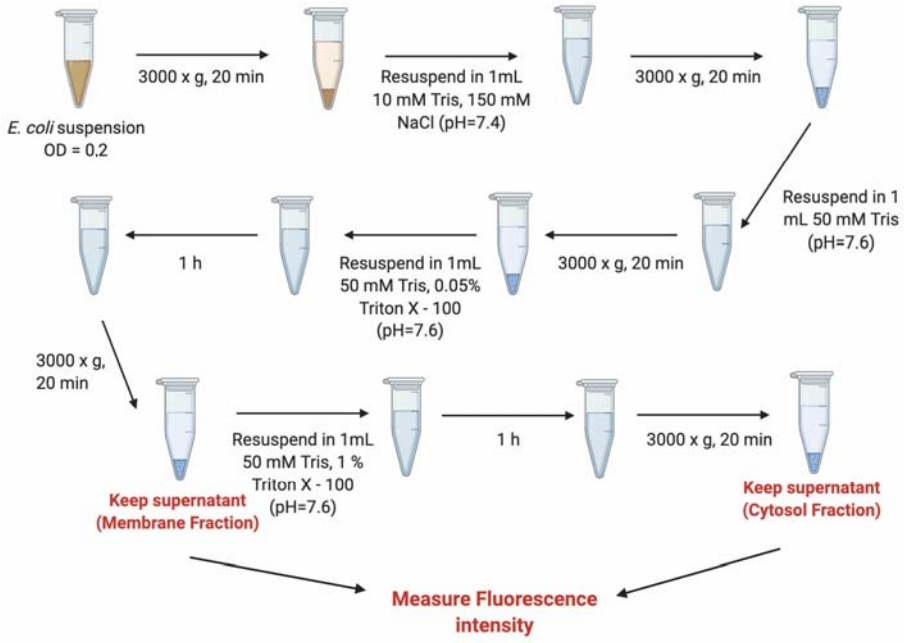


**Figure 6.** Fractionation protocol adapted from Bandula et al. [50]. A series of washing steps with a Triton X-100 gradient allows the isolation of the membrane and the cytosol fractions.

### *3.8. Statistical Analysis*

For the evaluation of the statistical significance, the two-way analysis of variance test (ANOVA) followed by Sydak's multiple comparisons was used. A *p*-value of $p \leq 0.05$ was considered statistically significant.

## 4. Conclusions

In summary, this innovative investigation discloses the challenges that need to be overcome before $B_{12}$ -mediated ASO internalization is considered realistic toward tackling

the challenge of antimicrobial resistance. This strategy is based on the uptake of the micronutrient $B_{12,}$ which seems to be insufficient to act as an efficient trojan-horse for ASOs designed to inhibit the expression of an essential bacterial gene. In the future, it would be relevant to assess the concentration of internalized ASOs needed to efficiently knock down bacterial genes and inhibit bacterial growth. In addition, improving the bioavailability of vitamin $B_{12}$ by modifying the conjugates and choosing better adapted bacterial targets would be important for successful translation from in vitro to in vivo application.

**Supplementary Materials:** The following are available online at https://www.mdpi.com/article/10.3390/antibiotics10040379/s1, Figure S1: Analytic RP-HPLC trace and MALDI-MS on $B_{12}$-ASOgapmer and $B_{12}$-$ASO_{steric}$. The top panel shows the retention time (in minutes) of the $B_{12}$ conjugates, and the bottom panel shows the mass (m/z) of each $B_{12}$ conjugate.; Figure S2: Interaction of Cy3 labeled ASOs, $B_{12,}$ and $B_{12}$ conjugates with *E. coli* K12, after 4 h incubation at a concentration of 15 µM. Bacteria are counterstained with DAPI. Images are representative of three independent experiments (using duplicates in each). Scale bar represents 5 µm; Figure S3: Most of the conjugated ($B_{12}$-$ASO_{steric}$) and unconjugated $B_{12}$ ($B_{12}$) are prevented from internalization into *E. coli* cytosol since they remain at the outer-membrane; the percentages in the periplasm are only residual. The isolation of the periplasm was performed after the isolation of the OM fraction and was based on the fractionation protocol by Malherbe et al. 2019. *E. coli* cells were washed in spheroplast buffer (0.1 M Tris-NaCl, 500 mM sucrose, 0.5 mM EDTA, pH 8.0) followed by resuspension in distilled water and incubation for 15 s on ice. The osmotic shock occurred after the addition of $MgSO_4$ (final concentration 20 mM). DAPI was used as a control, majorly localizing at the cytosol, as expected. Statistical differences are indicated when appropriate in * ($p \leq 0.0001$, ****); Table S1: Characterization of the synthesized conjugates, including their HPLC retention times ($t_R$) and molecular masses, as well as the yield of the respective conjugation reactions.

**Author Contributions:** Conceptualization, S.P., R.S.S., N.F.A., and J.W.; methodology, S.P., R.Y., P.T.J., J.W., N.F.A., and R.S.S.; experimental, S.P., M.G., and R.Y.; statistical analysis, S.P.; writing—original draft preparation, S.P. and R.S.S.; writing—review and editing, J.W.; N.F.A., P.T.J., M.G., and R.Y.; supervision, R.S.S., N.F.A., and J.W.; funding acquisition, N.F.A. and J.W. All authors have read and agreed to the published version of the manuscript.

**Funding:** The research was funded by Fundação para a Ciência e Tecnologia, PhD grant SFRH/BD/118018/2016; the Project UID/EQU/00511/2019-Laboratory for Process Engineering, Environment, Biotechnology and Energy–LEPABE funded by national funds through FCT/MCTES (PIDDAC); Project "LEPABE-2-ECO-INNOVATION"–NORTE-01-0145-FEDER-000005, funded by Norte Portugal Regional Operational Programme (NORTE 2020), under PORTUGAL 2020 Partnership Agreement, through the European Regional Development Fund (ERDF); and the European Union's Horizon 2020 research and innovation program under grant agreement No 810685; Biomolecular Nanoscale Engineering Center (BioNEC), a VILLUM center of excellence, funded by VILLUM FONDEN, grant number VKR18333.

**Institutional Review Board Statement:** Not applicable.

**Informed Consent Statement:** Not applicable.

**Data Availability Statement:** The data presented in this study are available in the article and in the supplementary material.

**Acknowledgments:** Joan Hansen and Tina Grubbe from BioNEC are thanked for technical assistance.

**Conflicts of Interest:** The authors declare no conflict of interest.

## References

1. Baker, S. A return to the pre-antimicrobial era? *Science* **2015**, *347*, 1064–1066. [CrossRef]
2. WHO. *The Evolving Threat of Antimicrobial Resistance: Options for Action*; World Health Organization: Geneva, Switzerland, 2012.
3. Pifer, R.; Greenberg, D.E. Antisense antibacterial compounds. *Transl. Res.* **2020**, *223*, 89–106. [CrossRef]
4. Bai, H.; You, Y.; Yan, H.; Meng, J.; Xue, X.; Hou, Z.; Zhou, Y.; Ma, X.; Sang, G.; Luo, X. Antisense inhibition of gene expression and growth in gram-negative bacteria by cell-penetrating peptide conjugates of peptide nucleic acids targeted to *rpoD* gene. *Biomaterials* **2012**, *33*, 659–667. [CrossRef]

5. Wengel, J. Synthesis of 3 '-C-and 4 '-C-branched oligodeoxynucleotides and the development of locked nucleic acid (LNA). *Acc. Chem. Res.* **1999**, *32*, 301–310. [CrossRef]
6. Giedyk, M.; Jackowska, A.; Równicki, M.; Kolanowska, M.; Trylska, J.; Gryko, D. Vitamin $B_{12}$ transports modified RNA into *E. coli* and *S. Typhimurium* cells. *Chem. Commun.* **2019**, *55*, 763–766. [CrossRef]
7. Geary, R.S.; Baker, B.F.; Crooke, S.T. Clinical and preclinical pharmacokinetics and pharmacodynamics of mipomersen (Kynamro®): A second-generation antisense oligonucleotide inhibitor of apolipoprotein B. *Clin. Pharmacokinet.* **2015**, *54*, 133–146. [CrossRef] [PubMed]
8. Kim, J.; Hu, C.; Moufawad El Achkar, C.; Black, L.E.; Douville, J.; Larson, A.; Pendergast, M.K.; Goldkind, S.F.; Lee, E.A.; Kuniholm, A. Patient-customized oligonucleotide therapy for a rare genetic disease. *N. Engl. J. Med.* **2019**, *381*, 1644–1652. [CrossRef] [PubMed]
9. Crooke, S.T. Molecular mechanisms of antisense oligonucleotides. *Nucleic Acid Ther.* **2017**, *27*, 70–77. [CrossRef] [PubMed]
10. Kole, R.; Krainer, A.R.; Altman, S. RNA therapeutics: Beyond RNA interference and antisense oligonucleotides. *Nat. Rev. Drug Discov.* **2012**, *11*, 125–140. [CrossRef] [PubMed]
11. Hegarty, J.P.; Krzeminski, J.; Sharma, A.K.; Guzman-Villanueva, D.; Weissig, V.; Stewart, D.B. Bolaamphiphile-based nanocomplex delivery of phosphorothioate gapmer antisense oligonucleotides as a treatment for *Clostridium difficile*. *Int. J. Nanomed.* **2016**, *11*, 3607. [CrossRef]
12. Turner, J.J.; Ivanova, G.D.; Verbeure, B.; Williams, D.; Arzumanov, A.A.; Abes, S.; Lebleu, B.; Gait, M.J. Cell-penetrating peptide conjugates of peptide nucleic acids (PNA) as inhibitors of HIV-1 Tat-dependent trans-activation in cells. *Nucleic Acids Res.* **2005**, *33*, 6837–6849. [CrossRef]
13. Järver, P.; Coursindel, T.; Andaloussi, S.E.; Godfrey, C.; Wood, M.J.; Gait, M.J. Peptide-mediated cell and in vivo delivery of antisense oligonucleotides and siRNA. *Mol. Ther. Nucleic Acids* **2012**, 1. [CrossRef]
14. Bennett, C.F.; Swayze, E.E. RNA targeting therapeutics: Molecular mechanisms of antisense oligonucleotides as a therapeutic platform. *Annu. Rev. Pharmacol. Toxicol.* **2010**, *50*, 259–293. [CrossRef]
15. Gruber, K.; Puffer, B.; Kräutler, B. Vitamin $B_{12}$-derivatives—enzyme cofactors and ligands of proteins and nucleic acids. *Chem. Soc. Rev.* **2011**, *40*, 4346–4363. [CrossRef] [PubMed]
16. Bassford, P.; Bradbeer, C.; Kadner, R.J.; Schnaitman, C.A. Transport of vitamin $B_{12}$ in *tonB* mutants of *Escherichia coli*. *J. Bacteriol.* **1976**, *128*, 242–247. [CrossRef] [PubMed]
17. Cadieux, N.; Phan, P.G.; Cafiso, D.S.; Kadner, R.J. Differential substrate-induced signaling through the TonB-dependent transporter BtuB. *Proc. Natl. Acad. Sci. USA* **2003**, *100*, 10688–10693. [CrossRef] [PubMed]
18. Giannella, R.; Broitman, S.; Zamcheck, N. Vitamin $B_{12}$ uptake by intestinal microorganisms: Mechanism and relevance to syndromes of intestinal bacterial overgrowth. *J. Clin. Investig.* **1971**, *50*, 1100–1107. [CrossRef] [PubMed]
19. Wierzba, A.; Wojciechowska, M.; Trylska, J.; Gryko, D. Vitamin $B_{12}$ suitably tailored for disulfide-based conjugation. *Bioconjugate Chem.* **2016**, *27*, 189–197. [CrossRef] [PubMed]
20. Chromiński, M.; Gryko, D. "Clickable" vitamin $B_{12}$ derivative. *Chem. A Eur. J.* **2013**, *19*, 5141–5148. [CrossRef] [PubMed]
21. Równicki, M.; Wojciechowska, M.; Wierzba, A.J.; Czarnecki, J.; Bartosik, D.; Gryko, D.; Trylska, J. Vitamin $B_{12}$ as a carrier of peptide nucleic acid (PNA) into bacterial cells. *Sci. Rep.* **2017**, *7*, 1–11. [CrossRef] [PubMed]
22. Rownicki, M.; Dąbrowska, Z.; Wojciechowska, M.; Wierzba, A.J.; Maximova, K.; Gryko, D.; Trylska, J.J.A.O. Inhibition of *Escherichia coli* growth by Vitamin $B_{12}$–Peptide Nucleic Acid Conjugates. *ACS Omega* **2019**, *4*, 819–824. [CrossRef]
23. Soares, N.C.; Spat, P.; Krug, K.; Macek, B. Global dynamics of the *Escherichia coli* proteome and phosphoproteome during growth in minimal medium. *J. Proteome Res.* **2013**, *12*, 2611–2621. [CrossRef] [PubMed]
24. Banerjee, D.; Shivapriya, P.; Gautam, P.K.; Misra, K.; Sahoo, A.K.; Samanta, S.K. A review on basic biology of bacterial biofilm infections and their treatments by nanotechnology-based approaches. *Proc. Natl. Acad. Sci.* **2020**, *90*, 243–259. [CrossRef]
25. Howard, J.J.; Sturge, C.R.; Moustafa, D.A.; Daly, S.M.; Marshall-Batty, K.R.; Felder, C.F.; Zamora, D.; Yabe-Gill, M.; Labandeira-Rey, M.; Bailey, S.M. Inhibition of *Pseudomonas aeruginosa* by peptide-conjugated phosphorodiamidate morpholino oligomers. *Antimicrob. Agents Chemother.* **2017**, 61. [CrossRef] [PubMed]
26. Narenji, H.; Teymournejad, O.; Rezaee, M.A.; Taghizadeh, S.; Mehramuz, B.; Aghazadeh, M.; Asgharzadeh, M.; Madhi, M.; Gholizadeh, P.; Ganbarov, K. Antisense peptide nucleic acids against *ftsZ* and *efaA* genes inhibit growth and biofilm formation of *Enterococcus faecalis*. *Microb. Pathog.* **2020**, *139*, 103907. [CrossRef]
27. Good, L.; Awasthi, S.K.; Dryselius, R.; Larsson, O.; Nielsen, P.E. Bactericidal antisense effects of peptide–PNA conjugates. *Nat. Biotechnol.* **2001**, *19*, 360. [CrossRef]
28. Lopez, C.; Arivett, B.A.; Actis, L.A.; Tolmasky, M.E. Inhibition of AAC (6′)-Ib-mediated resistance to amikacin in *Acinetobacter baumannii* by an antisense peptide-conjugated 2′, 4′-bridged nucleic acid-NC-DNA hybrid oligomer. *Antimicrob. Agents Chemother.* **2015**, *59*, 5798–5803. [CrossRef]
29. Azevedo, A.S.; Sousa, I.M.; Fernandes, R.M.; Azevedo, N.F.; Almeida, C. Optimizing locked nucleic acid/2′-O-methyl-RNA fluorescence *in situ* hybridization (LNA/2′OMe-FISH) procedure for bacterial detection. *PLoS ONE* **2019**, *14*, e0217689. [CrossRef]
30. Meng, J.; Wang, H.; Hou, Z.; Chen, T.; Fu, J.; Ma, X.; He, G.; Xue, X.; Jia, M.; Luo, X. Novel anion liposome-encapsulated antisense oligonucleotide restores susceptibility of methicillin-resistant Staphylococcus aureus and rescues mice from lethal sepsis by targeting *mecA*. *Antimicrob. Agents Chemother.* **2009**, *53*, 2871–2878. [CrossRef]

31. Xue, X.-Y.; Mao, X.-G.; Zhou, Y.; Chen, Z.; Hu, Y.; Hou, Z.; Li, M.-K.; Meng, J.-R.; Luo, X.-X. Advances in the delivery of antisense oligonucleotides for combating bacterial infectious diseases. *Nanomed. Nanotechnol. Biol. Med.* **2018**, *14*, 745–758. [CrossRef]
32. Meng, J.; Da, F.; Ma, X.; Wang, N.; Wang, Y.; Zhang, H.; Li, M.; Zhou, Y.; Xue, X.; Hou, Z. Antisense growth inhibition of methicillin-resistant *Staphylococcus aureus* by locked nucleic acid conjugated with cell-penetrating peptide as a novel *FtsZ* inhibitor. *Antimicrob. Agents Chemother.* **2015**, *59*, 914–922. [CrossRef] [PubMed]
33. Lou, C.; Martos-Maldonado, M.C.; Madsen, C.S.; Thomsen, R.P.; Midtgaard, S.R.; Christensen, N.J.; Kjems, J.; Thulstrup, P.W.; Wengel, J.; Jensen, K.J. Peptide–oligonucleotide conjugates as nanoscale building blocks for assembly of an artificial three-helix protein mimic. *Nat. Commun.* **2016**, *7*, 1–9. [CrossRef]
34. Dryselius, R.; Aswasti, S.K.; Rajarao, G.K.; Nielsen, P.E.; Good, L. The translation start codon region is sensitive to antisense PNA inhibition in *Escherichia coli*. *Oligonucleotides* **2003**, *13*, 427–433. [CrossRef] [PubMed]
35. Goltermann, L.; Yavari, N.; Zhang, M.; Ghosal, A.; Nielsen, P.E. PNA length restriction of antibacterial activity of peptide-PNA conjugates in *Escherichia coli* through effects of the inner membrane. *Front. Microbiol.* **2019**, *10*, 1032. [CrossRef] [PubMed]
36. Gottstein, C.; Wu, G.; Wong, B.J.; Zasadzinski, J.A. Precise quantification of nanoparticle internalization. *ACS Nano* **2013**, *7*, 4933–4945. [CrossRef]
37. Clais, S.; Boulet, G.; Kerstens, M.; Horemans, T.; Teughels, W.; Quirynen, M.; Lanckacker, E.; De Meester, I.; Lambeir, A.-M.; Delputte, P. Importance of biofilm formation and dipeptidyl peptidase IV for the pathogenicity of clinical *Porphyromonas gingivalis* isolates. *Pathog. Dis.* **2014**, *70*, 408–413. [CrossRef]
38. Malherbe, G.; Humphreys, D.P.; Davé, E. A robust fractionation method for protein subcellular localization studies in *Escherichia coli*. *Biotechniques* **2019**, *66*, 171–178. [CrossRef]
39. Zweifel, U.L.; Hagstrom, A. Total counts of marine bacteria include a large fraction of non-nucleoid-containing bacteria (ghosts). *Appl. Environ. Microbiol.* **1995**, *61*, 2180–2185. [CrossRef]
40. Kadner, R.J. Repression of synthesis of the vitamin $B_{12}$ receptor *in Escherichia coli*. *J. Bacteriol.* **1978**, *136*, 1050–1057. [CrossRef]
41. Davis, B.D.; Mingioli, E.S. Mutants of *Escherichia coli* requiring methionine or vitamin $B_{12}$. *J. Bacteriol.* **1950**, *60*, 17. [CrossRef]
42. Di Girolamo, P.M.; Kadner, R.J.; Bradbeer, C. Isolation of vitamin $B_{12}$ transport mutants of *Escherichia coli*. *J. Bacteriol.* **1971**, *106*, 751–757. [CrossRef]
43. Li, G.-W.; Burkhardt, D.; Gross, C.; Weissman, J.S. Quantifying absolute protein synthesis rates reveals principles underlying allocation of cellular resources. *Cell* **2014**, *157*, 624–635. [CrossRef] [PubMed]
44. Schembri, M.A.; Kjærgaard, K.; Klemm, P. Global gene expression in *Escherichia coli* biofilms. *Mol. Microbiol.* **2003**, *48*, 253–267. [CrossRef]
45. Soto, S.; Smithson, A.; Martinez, J.; Horcajada, J.; Mensa, J.; Vila, J. Biofilm formation in uropathogenic *Escherichia coli* strains: Relationship with prostatitis, urovirulence factors and antimicrobial resistance. *J. Urol.* **2007**, *177*, 365–368. [CrossRef] [PubMed]
46. Wexler, A.G.; Schofield, W.B.; Degnan, P.H.; Folta-Stogniew, E.; Barry, N.A.; Goodman, A.L. Human gut Bacteroides capture vitamin $B_{12}$ via cell surface-exposed lipoproteins. *Elife* **2018**, *7*, e37138. [CrossRef] [PubMed]
47. Good, L.; Sandberg, R.; Larsson, O.; Nielsen, P.E.; Wahlestedt, C. Antisense PNA effects in *Escherichia coli* are limited by the outer-membrane LPS layer. *Microbiology* **2000**, *146*, 2665–2670. [CrossRef] [PubMed]
48. Fontenete, S.; Guimarães, N.; Leite, M.; Figueiredo, C.; Wengel, J.; Azevedo, N.F. Hybridization-based detection of *Helicobacter pylori* at human body temperature using advanced locked nucleic acid (LNA) probes. *PLoS ONE* **2013**, *8*, e81230. [CrossRef] [PubMed]
49. Davis, B.D. Isolation of biochemically deficient mutants of bacteria by penicillin. *J. Am. Chem. Soc.* **1948**, *70*, 4267. [CrossRef] [PubMed]
50. Banbula, A.; Bugno, M.; Goldstein, J.; Yen, J.; Nelson, D.; Travis, J.; Potempa, J. Emerging Family of Proline-Specific Peptidases of *Porphyromonas gingivalis*: Purification and Characterization of Serine Dipeptidyl Peptidase, a Structural and Functional Homologue of Mammalian Prolyl Dipeptidyl Peptidase IV. *Infect. Immun.* **2000**, *68*, 1176–1182. [CrossRef]